

Spin and orbital magnetization in self-assembled Co clusters on Au(111)

H. A. Dürr, S. S. Dhesi, and E. Dudzik
Daresbury Laboratory, Warrington WA4 4AD, United Kingdom

D. Knabben
Institut für Angewandte Physik, Heinrich-Heine-Universität, D-40225 Düsseldorf, Germany

G. van der Laan
Daresbury Laboratory, Warrington WA4 4AD, United Kingdom

J. B. Goedkoop
European Synchrotron Radiation Facility, Boîte Postale 220, 38043 Grenoble, France

F. U. Hillebrecht
Institut für Angewandte Physik, Heinrich-Heine-Universität, D-40225 Düsseldorf, Germany
 (Received 7 October 1998)

We show that superparamagnetic Co clusters supported on a Au(111) surface exhibit a strong variation in perpendicular magnetic anisotropy with cluster size, which can be ascribed to electron localization at the perimeter of the clusters. The reduced dimensionality of such sites leads to drastic changes in the 3*d* electronic structure resulting in an increased orbital magnetic moment and a temperature-dependent 3*d* band occupancy. [S0163-1829(99)51202-2]

Miniaturization of magnetic materials can lead to unexpected and fascinating new phenomena, which are directly related to questions about the fundamental limits of information storage and the observation of macroscopic quantum phenomena. These investigations will ultimately provide new ways of using magnetic structures in technology. Quantum confinement, for instance, plays a crucial role in the giant magnetoresistance effect. Magnetic nanostructures represent model systems for the study of interesting physical phenomena that are due to the control of spatial dimensions of magnetic features at the microscopic scale. This opens up the investigation of finite-size effects on fundamental magnetic interactions. Spatial dimensions are coupled to temporal behavior and the dimensions determine the relative importance of different mechanisms for controlling the dynamics. Very important in future magnetic storage technologies is the superparamagnetic limit at which the inherent magnetic anisotropy of a small particle is no longer strong enough to produce a magnetization direction that is stable over the extended times¹ needed in nonvolatile magnetic memory.

Supported nanoscale clusters containing only 10^2 – 10^3 atoms are small enough to be in a single magnetic-domain state and even retain their magnetic moment above the bulk ordering temperature.² In the picture of classical magnetism the magnetic orientation of a small particle will remain stable below the blocking temperature. However, quantum tunneling gives rise to a coupling between the states in different potential wells, thereby leading to a completely different dynamics. In applications it is essential to be able to tailor the potential well and induce a magnetic anisotropy, preferably with an easy direction of magnetization perpendicular to the substrate surface. In this respect the orbital magnetic moment

m_L of the cluster is of great importance. For the heavy 3*d* transition metals it has been demonstrated that the easy direction of magnetization corresponds to the crystalline axis with the largest value of m_L .^{3–5} On the other hand, m_L is directly linked to the electronic structure and its size depends on the 3*d* hybridization and localization.⁶ For nanoscale clusters this can lead to interesting features. Finite system sizes may result in a significant energy narrowing of the valence electronic structure. In metallic systems the Fermi level intersects the valence levels so that changes in their thermal occupation result in a temperature dependence of m_L . Since the Hund's rule ground state has the largest orbital moment,⁷ we expect a reduction in the size of m_L with increasing temperature. This is not the case in bulklike metallic systems, where the valence levels conglomerate into bands. As a consequence, the orbital moment is strongly reduced and shows no significant variation with temperature. In the following we will demonstrate that nanoscale systems behave completely different compared to metallic bulk systems.

We chose Co clusters supported on an Au(111) single crystal surface as a model system. These clusters are self-assembled at the elbows of the Au(111) herringbone reconstruction during molecular-beam epitaxy at 300 K under ultrahigh vacuum conditions.⁸ Their morphology is well known from scanning tunneling microscopy studies. For Co coverages below an equivalent of $\Theta = 1$ atomic layers (AL) the clusters are of nearly circular shape 2 AL high.^{8,9} Above this coverage the individual clusters start to percolate,^{8,9} leading to structures with more fractal-like boundaries. Percolation also results in a rapid increase in the cluster size over a relatively narrow coverage range.⁹ The Au(111) surface was prepared by Ne ion bombardment and annealing to

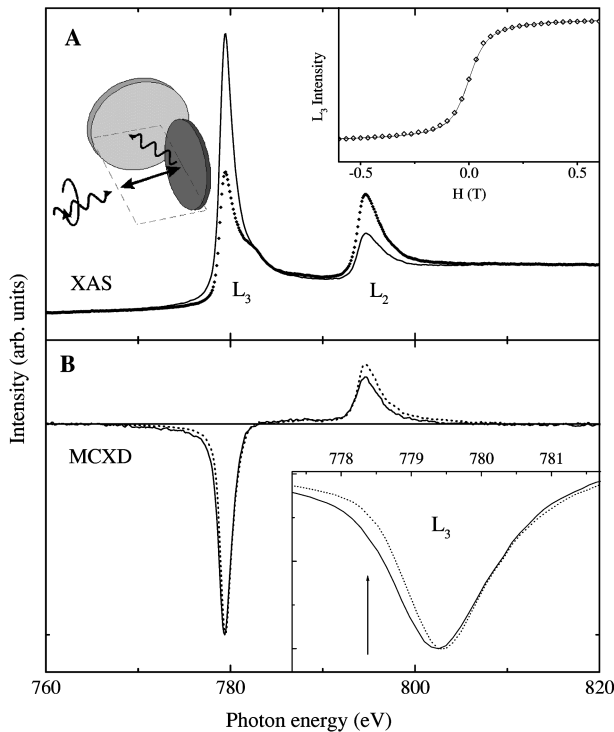


FIG. 1. XAS spectra measured with the photon spin parallel (line) and antiparallel (symbols) to the cluster magnetization. The Co spins were aligned by an external magnetic field of ± 4 T at a temperature of 20 K. The insets show the schematic experimental setup and the cluster magnetization as measured by the L_3 intensity variation versus the applied magnetic field (symbols). From the fitted Langevin function (solid line) the average cluster size can be obtained as 8000 ± 300 atoms. (b) Difference (MCXD) of the XAS spectra shown in (a) for 8000 atoms/cluster (dashed line) measured at 20 K and 300 atoms/cluster (solid line) measured at 10 K. The spectra were normalized to equal L_3 intensities. The change in the orbital moment is clear from the different areas of the L_2 edge (see text). The inset shows the expanded L_3 structures.

900 K.^{8,9} The Co deposition and subsequent measurements were carried out at pressures below 1×10^{-10} mbar to avoid surface contamination. Co coverages were measured with a quartz microbalance.

The magnetic characterization of the in-situ grown clusters was performed using magnetic circular x-ray dichroism (MCXD) at beamline ID12B of the European Synchrotron Radiation Facility in Grenoble. When the photon energy is swept across the spin-orbit split Co $L_{2,3}$ absorption edges, $2p$ core electrons are excited into unoccupied $3d$ valence states. The spin conservation in the absorption process aligns the spin of the $2p$ core hole with that of the magnetic $3d$ orbitals. Strong spin-orbit coupling in the core shell leads to an x-ray absorption spectroscopy (XAS) signal which depends on the relative alignment of photon spin and sample magnetization. This can be clearly seen in Fig. 1(a), where typical XAS spectra are shown for a Co coverage of 1.6 AL. The spectra were obtained with 85% circularly polarized photons by reversing the direction of the magnetic field of $H = \pm 4$ T. As shown in the left inset of Fig. 1(a), the x-ray beam was parallel to the magnetic-field direction with the sample tilted by 10° off normal incidence. The x-ray absorption cross section was measured by monitoring the fluorescence

yield (FY) of the $2p$ core-hole decay using a photo diode with an acceptance angle of 40° perpendicular to the incident light. The MCXD spectrum is the difference between the two XAS spectra, and the integrated intensities are related to the magnetic ground-state moments. Two typical difference spectra normalized to the L_3 intensity are shown in Fig. 1(b) for Co coverages corresponding to cluster sizes of $N = 8000$ (dashed line) and 300 atoms (solid line). From the integrated MCXD intensities $A_{2,3}$, at the corresponding edges the orbital moment per spin can be obtained as (Ref. 10) $m_L/m_S^{\text{eff}} = C_{\text{FY}} \frac{2}{3} (A_3 + A_2) / (A_3 - 2A_2)$. Here $m_S^{\text{eff}} = m_S + 7m_T$, where the magnetic dipole term m_T describes the anisotropy of the spin distribution which is less than 10–20% of m_S for Au/Co/Au(111) ultrathin films,⁴ so that it can be neglected here. The constant C_{FY} takes into account an energy-dependent decay probability for FY spectra that can lead to a deviation from the true XAS yield.¹¹ We determined $C_{\text{FY}} = 1.3$ for the larger clusters ($N > 8000$) by comparing the MCXD spectra obtained with FY and total electron yield. The latter is directly proportional to the absorption cross section,¹² but could only be employed for the large clusters due to the background signal from the Au(111) substrate. The FY correction factor was assumed to be independent of Co coverage. This seems justified since mainly the MCXD intensity at each absorption edge changes with Co coverage while the MCXD line shape remained almost unaffected. Small line-shape changes were found due to different occupied Co sites as discussed below. We found no evidence for saturation effects in the MCXD spectra due to the small Co coverages considered here.^{11,15}

For a precise determination of the cluster size we measured the sample magnetization monitored by the MCXD intensity of the L_3 absorption edge as a function of the applied magnetic field. The result for $\Theta = 1.6$ AL at a sample temperature of $T = 300$ K is shown in the right inset of Fig. 1(a) (symbols). At this temperature there is no remanent magnetization, the assembly of clusters is superparamagnetic, and the fluctuating total magnetic moments of the clusters can only be aligned by a strong external magnetic field. This behavior is described by the Langevin function,⁹ $I(L_3) \propto \coth(mNH/kT) - (mNH/kT)^{-1}$ where N is the average number of atoms per cluster and k is Boltzmann's constant. From the fit to the experiment [solid line in the right inset of Fig. 1(a)] we obtain $N = 8000 \pm 300$ atoms/cluster, assuming a bulk value of the total magnetic moment per atom of $m = 1.7\mu_B$.⁹ The values of N obtained at different temperatures in the superparamagnetic region were identical.

When the sample is cooled down below the so-called blocking temperature T_B , the anisotropy barrier between opposite magnetization directions can no longer be exceeded by thermal spin fluctuations.¹ A preferred spin direction is then selected by an external field, leading to a nonzero remanent macroscopic sample magnetization. T_B can be obtained from the onset of remanent magnetization M_0 by measuring hysteresis loops at different sample temperatures. Results are shown in the inset of Fig. 2(a) where M_0 is given normalized to the saturation magnetization M_S . We found a variation of T_B from 224 ± 10 K for $N = 12000 \pm 400$ atoms/cluster, to 30 ± 10 K for 300 ± 60 atoms/cluster. Although these values demonstrate a reduction of the absolute height

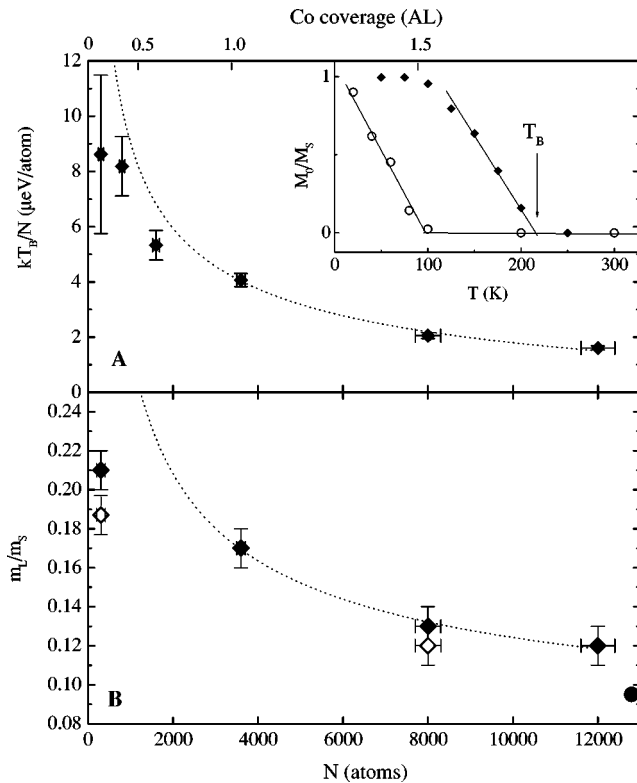


FIG. 2. Magnetic anisotropy barrier, $E_A \propto kT_B/N$, per cluster atom versus the number of atoms in a cluster, N (bottom axis) or the Co coverage (top axis). Note the nonlinearity of the bottom and top axes that indicates the rapid increase in N during cluster percolation. E_A was estimated from the blocking temperature T_B determined as shown in the inset. (b) Orbital magnetic moment per spin, r , versus cluster size. The solid diamonds represent measurements taken below T_B at temperatures of 10, 20, 20, and 100 K for 300, 3600, 8000, and 12 000 atoms/cluster, respectively. Above T_B , r was measured at 80 and 300 K for the 300 and 8000 atoms/cluster, respectively (open diamonds). The Co bulk value is given by the solid circle. The dashed lines represent a fit $\propto N^{-1/2}$ to the experimental data in both figures.

of the anisotropy barrier, the anisotropy energy per atom $E_A \propto kT_B/N$ actually increases when the cluster size is reduced [see Fig. 2(a)]. From angle-dependent MCXD spectra¹⁵ taken below T_B , we find that the easy magnetization direction is normal along the surface for all cluster sizes studied here, in agreement with earlier work.⁹

To investigate the microscopic origin of the enhancement in E_A we determined the Co orbital moment per spin, $r = m_L/m_S$. The results are summarized in Fig. 2(b) where r is given as a function of N for temperatures below (solid symbols) and above (open symbols) T_B . Shown are the averages of repeated MCXD measurements and their statistical uncertainties. While the value for the largest cluster size is identical to those obtained for ultrathin Au/Co/Au(111) sandwich films⁴ and slightly larger than the Co bulk value¹⁷ (solid circle), there is a clear increase in the values of r with decreasing cluster size. This is also apparent in the MCXD spectra of Fig. 1(b). A qualitatively similar tendency has been reported for the surface layer of epitaxial Co/Cu(100) films,⁶ and reflects the $3d$ band narrowing due to the reduced atomic coordination. In the case of clusters, the perimeter Co atoms have fewer neighbors compared to the center atoms.

Interatomic $3d$ hybridization is then less pronounced, leading to an increase in the orbital moment.

A further consequence of the reduction of $3d$ hybridization is a localization of the valence band electrons which results in modified energy levels for those Co atoms. This can be observed in XAS and MCXD as a change in excitation energy, which is visible as a photon energy shift of the $L_{2,3}$ absorption structures with cluster size. The inset of Fig. 1(b) clearly shows the photon energy shift between the 300 (solid line) and 8000 (dashed line) atoms/cluster MCXD data. However, more pronounced is the broadening of the L_3 absorption structure for the 300 atom clusters. This is caused by the appearance of a shifted component for the low-coordinated perimeter atoms [indicated by the arrow in the inset of Fig. 1(b)] at smaller photon energies compared to the center Co atoms.

More strongly localized valence electrons, and thus a reduced $3d$ band width, are expected to lead to changes in r depending on the temperature-dependent occupation of $3d$ orbitals near the Fermi level. We compared the temperature dependence of r for two cluster sizes, i.e., 300 and 8000 atoms/cluster. While for the latter, r is temperature independent within the experimental accuracy, there is a clear reduction of r with increasing temperature for the 300 atom clusters, as demonstrated by the solid and open symbols, respectively, in Fig. 2(b).

These results—(i) an enhanced orbital moment per spin r , (ii) shifts in the $L_{2,3}$ excitation energies, and (iii) a temperature-dependent variation of r —are manifestations of an increased $3d$ electron localization with reduced cluster size. The qualitatively similar variation of E_A [Fig. 2(a)] and r [Fig. 2(b)] with cluster size indicates the correlation of the two quantities. For a one-electron model of $3d$ transition metals it can be shown that the easy magnetization direction corresponds to the crystalline axis with the largest component of r .³ The observed increase in E_A can then be assigned to the $3d$ band narrowing in the smallest clusters which enhances r .⁶

It is generally believed that an increase of E_A is caused by the atomic sites with lowest coordination. Measurements on embedded Fe clusters were successfully interpreted within such a model, where only the relative changes in surface to volume with cluster size had to be taken into account.¹³ In the Co/Au(111) case we can distinguish mainly three inequivalent Co sites, i.e., atoms at the cluster perimeter, atoms at the Au, and atoms at the vacuum interfaces. Since the ratio of interface atoms and N is independent of cluster size, interface atoms cannot account for the observed changes in Fig. 2. For the perimeter Co atoms, on the other hand, we would expect a scaling of E_A and r with $fN^{-1/2}$ which is the relative number of perimeter sites in a cluster of size N . The factor f accounts for changes in the cluster shape. The dashed lines in Fig. 2 represent fits to the experimental data for constant f . This qualitatively describes the measurements. The observed deviation from the dashed lines in Fig. 2 is most likely caused by a change in the cluster morphology. While at low coverages the clusters are pancake-shaped ($f=1$), percolation above about 1 AL (Refs. 8 and 9) increases the relative number of perimeter atoms ($f>1$). For instance, a transition from circular to square-shaped islands would increase f by about 27%. The observation of a shifted

$L_{2,3}$ absorption structure for perimeter atoms provides additional evidence for this explanation, and perimeter sites indeed become more important at low coverages.

It is interesting that an increasing number of perimeter atoms with low coordination increases E_A , leading to uniaxial magnetic anisotropy with a preferred spin alignment perpendicular to the surface. The influence of steps on ultrathin fcc Co films is normally a stronger anisotropy in the surface plane parallel to the step edges.¹⁴ The microscopic origin for this behavior can be ascribed to the particular electronic valence band structure of the Co/Au(111) system. For 3d transition metals the effects of spin-orbit coupling causing a magnetic anisotropy can be described by a perturbation of the spin-polarized electronic structure.³ Perpendicular magnetic anisotropy is then introduced by L_z coupling between $3d_{zx}$ and $3d_{zy}$ or $3d_{xy}$ and $3d_{x^2-y^2}$ states straddling the Fermi level.^{3,16} L_z is the component of the orbital moment operator perpendicular to the surface (z axis). First-principles calculations for 1 AL Co/Au(111) point out the importance of the $3d_{zx}$ and $3d_{zy}$ electronic states which have their maximum electron density pointing towards and perpendicular to the Co nearest-neighbor direction (x axis), respectively.¹⁶ For a semi-infinite Co/Au(111) layer both types of orbitals have peaks in their respective density of states (DOS) above and below the Fermi level. The introduction of steps, which preferentially run along the close-packed atomic directions in the Co/Au(111) system, due to the formation of clusters is then expected to narrow the $3d_{zy}$ DOS of the perimeter Co atoms, thus shifting the maximum occu-

ried $3d_{zy}$ DOS closer to that of the less affected unoccupied $3d_{zx}$ states. This will increase both E_A and r (Ref. 16) as observed in our experiments.

The narrowing of the 3d band structure can also explain the observed temperature dependence of r for the smallest Co clusters. It is the temperature-dependent 3d level occupation near the Fermi level that reduces the value of r with increasing temperature. This is most likely due to an attenuation of m_L , since m_S was found to be almost temperature independent in gas phase experiments.² Because the size of r is a function of the 3d band width, its attenuation with temperature is far less pronounced for large clusters where r is only slightly larger than in the bulk¹⁷ [solid circle in Fig. 2(b)].

In conclusion we have studied the influence of cluster size and temperature on the orbital magnetic moment in nanoscale supported Co clusters. The increase of the perpendicular magnetic anisotropy barrier is a result of the reduced dimensionality at the cluster perimeter. This is evidenced by the observation of an energy shift in the 3d electronic levels of perimeter atoms and an increased orbital magnetic moment which is no longer temperature independent for small clusters. We hope that our results will lead to deepening of the microscopic understanding of the complex interplay between electron localization and orbital and spin ordering which is observed in materials such as colossal magnetoresistance oxides.

We thank N. B. Brookes, M. Finazzi, and K. Larsson for their help and technical assistance.

-
- ¹W. Wernsdorfer *et al.*, Phys. Rev. Lett. **78**, 1791 (1997).
²I. M. L. Billas, A. Châtelain, and W. de Heer, Science **265**, 1682 (1994).
³P. Bruno, Phys. Rev. B **39**, 865 (1989).
⁴D. Weller *et al.*, Phys. Rev. Lett. **75**, 3752 (1995).
⁵H. A. Dürr *et al.*, Science **277**, 213 (1997).
⁶M. Tischer *et al.*, Phys. Rev. Lett. **75**, 1602 (1995).
⁷O. Eriksson *et al.*, Phys. Rev. B **42**, R2707 (1990).
⁸B. Voigtländer, G. Meyer, and N. M. Amer, Phys. Rev. B **44**, 10 354 (1991).
⁹H. Takeshita *et al.*, J. Magn. Magn. Mater. **165**, 38 (1997).
¹⁰B. T. Thole, P. Carra, F. Sette, and G. van der Laan, Phys. Rev. Lett. **68**, 1943 (1992); P. Carra, B. T. Thole, M. Altarelli, and X. Wang, *ibid.* **70**, 694 (1993).
¹¹M. van Veenendaal, J. B. Goedkoop, and B. T. Thole, Phys. Rev. Lett. **77**, 1508 (1996).
¹²V. Chakarian, Y. U. Idzerda, and C. T. Chen, Phys. Rev. B **57**, 5312 (1998).
¹³F. Bodker, S. Morup, and S. Linderth, Phys. Rev. Lett. **72**, 282 (1994).
¹⁴R. K. Kawakami, E. J. Escorcia-Aparicio, and Z. Q. Qiu, Phys. Rev. Lett. **77**, 2570 (1996).
¹⁵W. L. O'Brien and B. P. Tonner, Phys. Rev. B **50**, 12 672 (1994).
¹⁶B. Ujfalussy, L. Szunyogh, P. Bruno, and P. Weinberger, Phys. Rev. Lett. **77**, 1805 (1996).
¹⁷C. T. Chen *et al.*, Phys. Rev. Lett. **75**, 152 (1995).